



# Lab on a Chip

**Mass-Producible Microporous Silicon Membranes for Specific Leukocyte Subset Isolation, Immunophenotyping, and Personalized Immunomodulatory Drug Screening *In Vitro***

Journal:	<i>Lab on a Chip</i>
Manuscript ID	LC-ART-04-2019-000315.R1
Article Type:	Paper
Date Submitted by the Author:	24-Jul-2019
Complete List of Authors:	Stephens, Andrew; University of Michigan, Mechanical Engineering Nidetz, Robert; University of Michigan, Mechanical Engineering Mesyngier, Nicolas; University of Michigan, Mechanical Engineering Chung, Meng Ting; University of Michigan Department of Mechanical Engineering, Song, Yujing; University of Michigan, Mechanical Engineering Fu, Jianping; Univ. of Michigan, Mechanical Engineering Kurabayashi, Katsuo ; University of Michigan, Mechanical Engineering

SCHOLARONE™  
Manuscripts

# **Mass-Produced Microporous Silicon Membranes for Specific Leukocyte Subset Isolation, Immunophenotyping, and Personalized Immunomodulatory Drug Screening *In Vitro***

Andrew Stephens<sup>\*a</sup>, Robert Nidetz<sup>\*a</sup>, Nicolas Mesyngier<sup>a</sup>, Meng Ting Chung<sup>a</sup>, Yujing Song<sup>a</sup>, Jianping Fu<sup>ab</sup>, and Katsuo Kurabayashi<sup>ac</sup>

<sup>a</sup>Department of Mechanical Engineering, University of Michigan, Ann Arbor, Michigan, 48109, USA.

<sup>b</sup>Department of Biomedical Engineering, University of Michigan, Ann Arbor, Michigan, 48109, USA.

<sup>c</sup>Department of Electrical Engineering and Computer Science, University of Michigan, Ann Arbor, Michigan, 48109, USA. E-mail: [katsuo@umich.edu](mailto:katsuo@umich.edu)

\*These authors contributed equally to this work.

## ABSTRACT

Widespread commercial and clinical adaptation of biomedical microfluidic technology has been limited in large part due to the lack of mass producibility of polydimethylsiloxane (PDMS) and glass-based devices commonly as reported in the literature. Here, we present a batch-fabricated, robust, and mass-producible immunophenotyping microfluidic device using silicon micromachining processes. Our Si and glass-based microfluidic device, named the silicon microfluidic immunophenotyping assay (SiMIPA), consists of a highly porous (~ 40%) silicon membrane that can selectively separate microparticles below a certain size threshold. The device is capable of isolating and stimulating specific leukocyte populations, and allows for measuring their secretion of cell signaling proteins by means of a no-wash homogeneous chemiluminescence-based immunoassay. The high manufacturing throughput (~ 170 devices per wafer) makes a large quantity of SiMIPA chips readily available for clinically relevant applications, which normally require large dataset acquisitions for statistical accuracy. With 30 SiMIPA chips, we performed in-vitro immunomodulatory drug screening on isolated leukocyte subsets, yielding 5 data points at 6 drug concentrations. Furthermore, the excellent structural integrity of the device allowed for samples and reagents to be loaded using a micropipette, greatly simplifying the experimental protocol.

## INTRODUCTION

Solid organ transplant recipients are routinely prescribed immunosuppressive drugs in order to prevent allograft rejection. Allograft rejection is the result of the host's T-cells recognizing and signaling the host to mount an immune response against the transplant, resulting in graft failure. Tacrolimus, a calcinurine inhibitor, is commonly prescribed as part of an immunosuppressive drug regimen to prevent transplant rejection in the host. Tacrolimus prevents activation of T-cells by disrupting the calcinurine/nuclear factor of activated T-cells (NFAT) pathway<sup>1</sup>, which prevents the host's T-cells from producing inflammatory biomarkers and initiating graft rejection. However, tacrolimus has a narrow therapeutic window and dosing remains challenging.<sup>1</sup> If tacrolimus is underdosed, the immune response of the patient will not be sufficiently suppressed to prevent acute rejection.<sup>2</sup> Over-administering tacrolimus has been shown to lead to renal dysfunction, opportunistic infection, and metabolic disorders.<sup>3</sup> Furthermore, recent research has shown that the immune system's response to tacrolimus (sufficient vs. insufficient suppression) can vary in a group of patients given otherwise identical drug regimens<sup>4</sup>. Therefore, there exists a need to assess a personalized minimal dosage of tacrolimus that will prevent allograft rejection while still allowing the immune system to fight pathogenic infection.<sup>3</sup> Functional immunophenotyping – the quantification of secreted cytokines, such as IL-2 – of T-cells provides the means to assess the efficacy of tacrolimus in preventing the risks of allograft rejection.<sup>4,5</sup>

Functional immunophenotyping is conventionally achieved by enzyme linked immunosorbent assay (ELISA), enzyme linked immunosorbent spot (ELISpot) or intracellular cytokine staining (ICS) flow cytometry. ELISA/ELISpot techniques are the current gold-standard for quantifying cellular cytokine production, however, the complexity of these techniques limits their use in rapid patient immune status assessment and in the specific components of the immune

response that can be monitored in a single run. For ELISA, common practice is to collect the supernatant of the cell population being studied and perform the assay on small amounts of the supernatant in individual wells of a polystyrene well plate. The interior surfaces of the wells are functionalized with “capture” antibodies that selectively bind to the cytokine to be quantified then subsequently labeled with a secondary antibody linked to an enzyme. The enzyme’s substrate is added to the well. A color change in the liquid in the well is produced and correlated to the concentration of cytokine in the sample. Between these steps, the ELISA assay requires several washing and incubation procedures to ensure assay specificity and antibody-antigen binding. Involving these cumbersome procedures, ELISA is normally time consuming and laborious. The ELISpot assay is performed by adding a cell population to a culture plate functionalized with antibodies targeting the cytokine of interest. Incubated in the culture plate, the cells secrete cytokines. These cytokines are captured by antibodies near the cells. After the cells are washed away, a secondary antibody with a linked enzyme is added to the plate. With the enzyme’s substrate added, a color change is locally produced in areas that had cytokine-secreting cells. These areas appear as spots under a microscope and the spots are then counted to determine the number of cytokine-producing cells in the population. The throughput of the ELISpot assay is similarly limited as ELISA by time-consuming incubation and washing steps. The ELISpot assay commonly takes 2 or more days depending on the incubation time required. ELISpot is inherently more sensitive than ELISA as the analyte is detected very close to the cell rather than diluted in the bulk medium, however, ELISpot assay provides only the fraction of cells producing the cytokine of interest rather than the quantity of cytokine produced. Both ELISA/ELISpot assays only provide information of the overall secretomic activity of the entire sample population being studied. Unless the sample is pre-processed using fluorescence activated cell sorting (FACS) or other cell sorting

technique, ELISA/ELISpot cannot determine the activity of a phenotypic cell subset. Use of FACS greatly increases the complexity of experimental setup and requires a sophisticated flow cytometry system as well as highly trained operators. Cell subset or single-cell functional immunophenotyping can be achieved using ICS flow cytometry at high throughput. However, this technique also requires a sophisticated flow cytometry system and highly skilled operators. The complexity of ICS protocol, often highly laboratory-specific, limit the technique's implementation when considering multicenter clinical studies.<sup>6</sup>

Integrative and sample-sparing microfluidic solutions have been developed to overcome the shortcomings of conventional functional immunophenotyping techniques.<sup>7</sup> Immunophenotyping of T-cells requires isolating T-cells from whole blood, stimulating the isolated cells, and quantifying the secreted cytokines. Recently, researchers have demonstrated isolating specific immune cells from whole blood using microfluidics for subsequent analysis.<sup>4,8-11</sup> Various techniques have been employed to isolate these cells which can take advantage of cellular biomarkers (i.e. fluorescent tagging and bead binding) or the physical properties of the cells (i.e. inertial separation and size filtration).<sup>12,13</sup> Recently, our lab developed a PDMS-based microfluidic immunophenotyping assay (MIPA) that integrated all sorting, stimulation, and assay components of monocyte functional immunophenotyping.<sup>9,11</sup> The MIPA device utilized a micromachined filtration membrane to precisely isolate particles flowed through the device based on their size. Integrating sorting, stimulation, and assay components greatly reduced the complexity required because it eliminated the need for pre-processing with FACS and separate ELISA/ELISpot assay. However, the fabrication process of the MIPA device required laborious manual assembly of very delicate components, limiting its manufacturing throughput and the overall experimental throughput of the technique. A single MIPA device could only be used to

perform one immunophenotyping measurement and was subsequently discarded. Indeed, manufacturability poses a significant challenge to widespread dissemination of many PDMS-based microfluidic devices.<sup>14–16</sup>

Here, we have developed a silicon-based microfluidic immunophenotyping assay (SiMIPA) manufactured using silicon micromachining processes. The use of Si microfluidics overcomes challenges in manufacturing and scaling up traditional PDMS-and-glass based microfluidics which have prohibited their wide adaptation in industry. The design concept of the device was adapted from our previous device solely made of polydimethylsiloxane (PDMS) and glass.<sup>9,11</sup> The new SiMIPA device is made up of four components: PDMS microfluidic chamber, microfiltration membrane, immunoassay chamber, and a transparent glass layer (Fig. 1a). The PDMS microfluidic chamber guides a biological sample through the microfiltration membrane, which filters out particles that are too large to pass through its 20  $\mu\text{m}$  diameter pores. The immunoassay chamber provides sufficient fluidic volume to perform an on-chip homogeneous chemiluminescence-based immunoassay. Light is permitted to pass into the immunoassay chamber by the transparent glass layer. The Si micromachining processes developed for the SiMIPA device enables wafer-level batch fabrication, batch-to-batch uniformity, and manufacturing throughput of 172 SiMIPA devices (8.8 mm x 4.3 mm die size) per 100 mm SOI wafer with >99% yield. Additionally, the comparatively much higher yield strength of the Si filtration membrane<sup>17</sup> allows for sample and reagent loading into the device using a handheld micropipette instead of a syringe pump, greatly simplifying the experiment protocol.

The manufacturing and handling improvements to the device enables greater experimental throughput of the MIPA technique, allowing for comprehensive assessment of T-cell functional response following exposure to the immunosuppressive drug tacrolimus. In this work, we use the

SiMIPA device to selectively isolate T-cells from a heterogeneous mixture and perform subsequent functional immunophenotyping. T-cell isolation is achieved by mixing the sample with anti-CD3 coated polystyrene (CD3-PS) beads prior to sample loading into the device. The CD3-PS beads selectively bind to the T-cells in a sample and, when the sample is loaded into the device, are caught by the microporous Si membrane on the SiMIPA device where they remain mechanically fixed throughout the experiment. We evaluate the performance of the SiMIPA technique in terms of its limit of detection of cell-secreted cytokines, number of cells required per assay, and total assay time. Immunomodulatory drug screening *in vitro* is achieved by isolating CD3+ Jurkat T-cells in SiMIPA devices that had been cultured in medium containing a known concentration of tacrolimus. After isolation, the CD3+ Jurkat cells are chemically stimulated to secrete cytokines and a bead-based, biological assay, AlphaLISA, is used to quantify the secretion of IL-2 on-chip. From just 1 mL of sample, we were able to assess the functional cellular response to 5 concentrations of tacrolimus plus negative control with  $n = 5$ , which required 30 single-use SiMIPA devices and was performed in a single day. Thus, we have enabled the potential use of the SiMIPA device in clinical study towards personalized immunotherapy.

## MATERIALS AND METHODS

### *SiMIPA chip microfabrication*

The SiMIPA was fabricated using silicon micromachining processes (Fig. S1). First, a SOI wafer (50  $\mu\text{m}$ /0.5  $\mu\text{m}$ /525  $\mu\text{m}$ /2  $\mu\text{m}$ , device/BOX/handle/handle oxide thickness, Ultrasil LLC, Hayward, CA) was cleaned in piranha solution (3:1 v/v  $\text{H}_2\text{SO}_4$  :  $\text{H}_2\text{O}_2$ ), the handle layer oxide of the wafer was patterned using photolithography, etched using reactive ion etching (RIE) to define a hard mask for the cavity etch, and piranha-cleaned again. Subsequently, photolithography was

used to define a 3 x 3 mm<sup>2</sup> array of holes (20 μm diameter, 30 μm center-to-center spacing, hexagonal lattice) for each chip on the device layer which would serve as the microfiltration membrane. Deep reactive ion etching (DRIE, ~17 μm/min etch rate, Pegasus 4, SPTS) was used to etch the hole pattern to the buried oxide layer (BOX). After stripping the photoresist, the SOI wafer was mounted onto a 100 mm diameter Si carrier wafer using Crystalbond 555 (Aremco Products, Valley Cottage, NY). The cavity was then etched into the handle layer with DRIE to the BOX layer across the whole wafer. The SOI wafer was then carefully dismantled from the carrier wafer and thoroughly cleaned to remove all Crystalbond. Following an O<sub>2</sub> descum, the remaining SiO<sub>2</sub> hard mask and BOX were etched away using BHF. After piranha cleaning the SOI wafer and a borofloat glass wafer, anodic bonding (SB-6e, Suss Microtec, Germany) was used to bond the glass to the handle layer, sealing the cavity. The bonded wafers were then diced (ADT 7100 Dicing Saw, Advanced Dicing Technologies, Israel) into 172 individual SiMIPA chips.

Separately, the top PDMS chamber of the SiMIPA was created using a soft lithography technique. In brief, a ~100 μm deep Si mold was first formed within a wafer using photolithography and deep reactive ion etch (DRIE). The Si wafer mold was then coated with (tridecafluoro-1,1,2,2,-tetrahydrooctyl)-1-trichlorosilane (United Chemical Technologies) to facilitate the subsequent release of the PDMS from the Si mold. A prepolymer (Sylgard 184, Dow Corning) was then poured onto the Si wafer mold and degassed under house vacuum for a few hours to remove any bubbles. After degassing, the prepolymer was allowed to cure overnight on a level bench top and then baked for 3 hours in a 60 °C oven to complete the polymerization. The PDMS was then carefully removed from the mold and cut into individual devices with a razor blade. 1 mm diameter holes were punched in the PDMS using a biopsy punch to create the inlet

and outlet. Up to 28 PDMS pieces for the top chamber could be produced from a 100 mm diameter Si wafer.

After removing individual SiMIPA chips from the dicing tape, the devices were treated with O<sub>2</sub> plasma and piranha cleaned to remove organics and minerals from the SiMIPA chips. After copious rinsing in DI water, the SiMIPA chips were stored in DI water until ready for PDMS bonding. Prior to PDMS bonding, the SiMIPA chips were placed on a hotplate set to 110 °C until dry. The SiMIPA chips were placed in a custom, machined, aluminum jig and then the SiMIPA chips and PDMS were treated with O<sub>2</sub> plasma (50 W, 100% O<sub>2</sub>, 0.7 Torr, 60 sec, Covance, Femto Science, South Korea) to activate the Si and PDMS surfaces for bonding. The PDMS was manually aligned to the SiMIPA chip, allowed to initiate contact, and then stored overnight to ensure a strong interfacial bond.

### ***Cell Culture***

Jurkat cells (TIB-152, ATCC) were cultured in RPMI-1640 (ATCC 30-2001) growth medium supplemented with 10% (v/v) fetal bovine serum (FBS) (ATCC 30-2020) and 100 U/mL Penicillin-Streptomycin (ThermoFisher). THP-1 cells (TIB-202, ATCC) were cultured separately using the same formulation of growth medium. All cell cultures were incubated at 37°C and 100% humidity in a CO<sub>2</sub> cell culture incubator (Thermo Scientific). Every 2-3 days, cell culture medium for all cultures was replaced by centrifuging the cells at 1200 RPM for 5 minutes, removing the supernatant, and resuspending the cells in fresh growth medium. The concentration of cells for all cell cultures was maintained at  $2 \times 10^5 - 2 \times 10^6$  cells/mL.

### ***Preparation of Devices Prior to Use.***

Assembled devices were treated with O<sub>2</sub> plasma, filled with DI water, and placed under low vacuum to completely degas the device. After degassing, the SiMIPA devices were submerged in DI water in a sealed dish and stored at 3 °C for future use. Immediately before use, devices were flushed with 50 µL of blocking buffer (SuperBlock, Thermo Scientific) to prevent nonspecific binding of proteins and cells to the interior surfaces of the SiMIPA devices. Devices were allowed to incubate for 1 hour at room temperature, after which they were flushed with 75 µL of cell culture medium. This preparation step was performed for all devices used in the present study.

### ***Isolation of Specific Immune Cell Subpopulations In-Device and Evaluation of Isolation Purity***

Jurkat and THP-1 cells were taken from culture and transferred to separate centrifuge tubes. The concentration of both cell types was adjusted to  $2 \times 10^6$  cells/mL by centrifugation at 1200 RPM for 5 minutes and resuspended in fresh medium. The final volume of each was 1 mL. The Jurkat cells were then stained with Calcein AM Green (Invitrogen) and the THP-1 cells were stained with Calcein AM Red-Orange (Invitrogen). Excess dye was washed from both samples by centrifugation, removing the supernatant, and adding fresh medium for a total of 3 washes. The Jurkat and THP-1 cells were then combined to create a mixture of the two cell lines with a concentration of  $2 \times 10^6$  cells/mL Jurkat cells and  $2 \times 10^6$  cells/mL THP-1 cells, with a volume of 1 mL. Subsequently, 80 µL stock solution of anti-CD3 coated polystyrene beads (CD3-PS beads,  $2.5 \times 10^6$  beads/mL, CD3 S-pluriBead, anti-human, 32 µm diameter, pluriSelect, Germany) was added to the cell mixture and mixed on a roller mixer (pluriSelect, Germany) for 30 minutes at 15 RPM, allowed to rest for 15 minutes, and then mixed again for 15 minutes.

After mixing, the bead and cell solution was diluted 4x and 40 µL was pipetted into the inlet of a prepared SiMIPA device. The device was then washed with 75 µL of culture medium to

remove cells not bound to CD3-PS beads. Glass coverslips were placed at the inlet and outlet of the device to prevent cells or beads from escaping after washing. The cells and beads isolated on the microporous membrane of the SiMIPA device were imaged using an inverted fluorescence microscope (Nikon Eclipse Ti) and an electron multiplying CCD (EMCCD, Photometrics, Tucson, AZ). Separately, 10  $\mu\text{L}$  of the cell and bead mixture was spread on a hemacytometer and imaged with the fluorescence microscope and EMCCD. In all cases bright field and fluorescence images were acquired. The images were analyzed using the ImageJ (NIH) multipoint tool in order to count the number of beads and the number of cells bound to the beads.

### ***Quantification of T Cell-Secreted Cytokines using SiMIPA***

Jurkat cells were taken from culture and centrifuged at 1200 RPM for 5 minutes. The supernatant was removed and the cells were resuspended in fresh medium. The concentration of Jurkat cells was adjusted to  $2 \times 10^6$  cells/mL. Then, 80  $\mu\text{L}$  of CD3-PS beads (pluriSelect) stock solution was added to 1 mL of Jurkat cells at  $2 \times 10^6$  cells/mL in a microcentrifuge tube. The cells and beads were then mixed on a roller mixer as previously described. Then, 4.05 – 32.4  $\mu\text{L}$  of the cell-bead mixture (depending on the experiment) was injected into the inlet of a SiMIPA device using a handheld micropipette. The SiMIPA device was then flushed with 75  $\mu\text{L}$  of a cocktail containing cell culture medium, 100/1000 ng/mL *para*-methoxyamphetamine/inomycin (PMA/Io), and tacrolimus. The device was then immediately placed in a cell culture incubator and allowed to incubate for the time required by the experiment.

The quantification of cytokine molecules secreted by T cells conjugated with beads trapped on the Si membrane of the device was performed by AlphaLISA (Perkin Elmer AL33C), a no-wash, homogeneous bead-based sandwich immunoassay technique. The AlphaLISA technique

involves the measurement of laser ( $\lambda = 680$  nm at 500 mW)-induced chemiluminescence between pairs of antibody-conjugated donor and acceptor beads (250–350 nm in diameter) in close proximity to each other in the presence of a sandwiched analyte molecule. A single SiMIPA device was placed in the path of the objective lens of a custom optical setup (Fig. S2). Laser light was guided by the objective lens through the transparent backside glass layer of the SiMIPA device. The laser exposure lasted for 500 ms and was controlled using a shutter (Lambda SC, Sutter Instrument Co.) via LabView. For the next 500 ms, after closing the excitation shutter, LabView controlled shutter was opened to allow 615 nm light emitted by the acceptor beads to be quantified using a photomultiplier tube (PMT, H9306-03, Hamamatsu, Japan). The collection shutter was closed and after a 4.6 second rest the excitation and collection were repeated and the data was output to file. In addition to controlling the shutters and collecting the data from the PMT, the LabView program also controlled the gain on the PMT.

### ***Finite element modeling the deflection of the microporous membrane under fluidic flow***

Finite element modeling software (COMSOL 5.3 Multiphysics, COMSOL, Inc.) was used to predict the deflection of the microporous membrane and accompanying stress under fluidic flow. A  $3 \times 3 \times 0.05$  mm<sup>3</sup> Si membrane was drawn in SolidWorks (Dassault Systèmes) and imported into COMSOL. To simplify the model and ensure efficient computation, only one quadrant of the membrane was simulated and symmetric boundary conditions were applied to the edges of the model. Later, the mirroring feature in COMSOL was used to reconstruct the entire membrane. A stationary study using the solid mechanics model was used where the four  $3 \times 0.05$  mm<sup>2</sup> sides of the membrane were constrained and a pressure was applied to the top  $3 \times 3$  mm<sup>2</sup>

surface of the membrane. Previous work showed that the pressure drop ( $\Delta P$ ) across a circular-pore membrane filter to be

$$\Delta P = \left( \frac{128L\mu}{\pi d^4} + \frac{24\mu}{d^3} \right) \frac{Q}{N} f_i(k), \quad (1)$$

where  $L$  is the pore depth,  $d$  is the pore diameter,  $N$  is the number of pores,  $\mu$  is the coefficient of dynamic viscosity,  $Q$  is the flow rate,  $k$  is the fraction of open area of the pores, and the function  $f_i(k)$  is defined as:

$$f_i(k) = 1 - \sum_{i=1}^{\infty} a_i k^{(i+1)/2}, \quad (2)$$

where  $a_1 = 0.344$ ,  $a_2 = 0.111$ , and  $a_3 = 0.066$ .<sup>18</sup>**Error! Reference source not found.** The microporous membrane in the SiMIPA device has 11,443 pores which are 20  $\mu\text{m}$  in diameter, 50  $\mu\text{m}$  deep, and provide a total porosity of 39.94%. Assuming that the medium is water ( $\mu = 0.1 \text{ Pa s}$ ),

$$\Delta P = Q \times 1.133 \times 10^{11} \frac{\text{Pa} \cdot \text{s}}{\text{m}^3}. \quad (3)$$

For flow rates of 10, 100, and 1000  $\mu\text{L/s}$ , the pressure drop is 1.133, 11.33, and 113.3 kPa, respectively. When the membrane is loaded with 6000 beads, approximately half the holes are clogged and  $N$  is halved, thus doubling the effective pressure drops to 2.266, 22.66, and 226.6 kPa for flow rates of 10, 100, and 1000  $\mu\text{L/s}$ , respectively. This is equivalent to doubling the flow rate,

as Eq. 1 shows that  $Q/(N/2) = 2Q/N$ . A parametric sweep was used to model membrane deflection and von Mises stresses for different flow rates for the conditions of no beads and 6000 beads.

## RESULTS AND DISCUSSION

### Enhanced device manufacturability, reliability, design, and handling

Fig. 2 details the features of the SiMIPA. The manufacturing methods of SiMIPA device enabled significantly greater manufacturing throughput, and thereby experimental throughput, versus the previous PDMS-based MIPA device. By switching from an entirely PDMS and glass design to Si, glass, and PDMS (Fig. 2a), key manufacturing bottlenecks were eliminated. The first and most limiting bottleneck of the previous device was low yield of the PDMS membrane layer.<sup>9,11,19</sup> After photolithographic patterning, the 10  $\mu\text{m}$  thick PDMS membrane was extremely delicate and prone to tearing during separation from the Si wafer mold, resulting in a yield of only about 20-40%, or 11-22 devices, per 100 mm Si wafer. Furthermore, the membrane in the previous device was subject to unpredictable rupture during usage or the membrane deflecting until it collapsed and irreversibly stuck to the bottom chamber, making the actual yield far lower. In contrast, the Si membrane layer of the SiMIPA device, imaged in Fig. 2b, needed no such separation step, could be fabricated with >99% yield, and the membrane never failed during usage. A fully processed wafer, with 172 chips, is shown in Fig. 2c. Second, the number of manual alignment and assembly steps were decreased from two to one in the SiMIPA platform. The PDMS MIPA required two manual alignment steps to stack the PDMS layers together to correctly assemble the device, with a misalignment resulting in scrapping the device and thus decreasing overall yield. In the SiMIPA device, only one such manual alignment step was needed to bond the PDMS top layer to the membrane layer. A completed device is shown in Fig. 2c. Decreasing the

number of PDMS assembly steps compared to the previous device design also reduced the manufacturing time by only requiring one O<sub>2</sub> plasma bonding step. Overall, we estimate that the fabrication of the SiMIPA device was 6 min/device, while the PDMS MIPA required 30 min/device.

By using Si instead of PDMS, the SiMIPA minimizes dead volume. The PDMS MIPA and other PDMS-based microfluidic blood filtration devices required support posts for the microfiltration membrane to prevent the PDMS membrane from deforming and even rupturing under fluid flow.<sup>9,11,20</sup> Because Si has a much higher Young's modulus than PDMS (170 GPa vs 750 kPa, respectively), rapid flow rates (>100 μL/sec via micropipette) could be used with only minimal deflection and without damaging of the free-standing membrane despite its nearly 40% porosity. The integrity of the membrane was tested at flow rates up to 20 mL/min and no deflection or damage could be observed using an optical microscope. The membrane remained intact even when rapidly dispensing 1 mL into the inlet of the device using a handheld micropipette.

We machined aluminum jigs in order to facilitate the PDMS bonding of multiple SiMIPA chips at the same time in order to maximize throughput. Although the jig has spots for eight SiMIPA chips, a maximum of four SiMIPA chips were used at one time. This was because the shrinkage of the PDMS after removal from the master mold averaged  $1.32 \pm 0.12$  %, similar to what has been previously reported.<sup>21</sup> While the master mold was designed to adjust for the 1.32% shrinkage, the standard deviation compounded to provide too much misalignment for O<sub>2</sub> plasma bonding more than four SiMIPA chips at a time. Throughput at this manual assembly step could be improved with strictly controlled PDMS preparation and molding, PDMS bonding with the assistance of robotics, or by entirely replacing the PDMS layer with a material that could be molded and bonded to the Si device layer, such as polystyrene or glass. Indeed, PDMS is inherently

not suited to mass manufacturing<sup>14,22</sup>, but was preferred here in order to enable compatibility with a wide range of laboratory tools, especially the handheld micropipette. Specialized interfaces for sample loading and interface with measurement system are advantageous in commercial microfluidic systems, such as the 10x Genomics Chromium Controller, for highly specialized applications. These approaches were considered cost-prohibitive and not implemented for the SiMIPA device as the throughput was more than sufficient for the application presented here, but are readily implemented if the device were to be commercialized.

We manufactured custom 3 x 2 in<sup>2</sup> acrylic slides featuring slots for six SiMIPA devices (Fig. S4) using a laser cutter. The purpose of the slides was two-fold. First, it standardized the locations of the SiMIPA devices on the microscope stage for imaging and quantifying the cytokine secretion with the AlphaLISA kits. Second, the slides provided mechanical stability for the SiMIPA devices during handling. Initially, the PDMS had the same foot print as the SiMIPA chip. This made the SiMIPA devices difficult to handle because they were top heavy and tended to tip over during pipetting and when the pipette tips were left in the device. By enlarging the PDMS so that it was twice as wide and long as the SiMIPA chip, the SiMIPA device could be impermanently mounted on the acrylic slides and the devices would no longer tip over.

### ***Finite element modeling the deflection of the microporous membrane under fluidic flow***

The results of the simulated defection of the membrane under fluidic flow are shown in Fig. 3. The simulation of the full 3 x 3 x 0.05 mm<sup>3</sup> Si membrane was simplified by invoking symmetrical boundary conditions along the axes of the x-y plane (origin in the center of the membrane) such that only one-quarter of the membrane needed to be simulated. The deflection profile of the entire membrane was reconstructed using the mirroring feature in COMSOL.

Fig. 3a shows the simulated deflection of the Si membrane under 2000  $\mu\text{L/s}$  flow rate, which is equivalent to the condition where the flow rate is 1000  $\mu\text{L/s}$  but half the pores are clogged. The maximum deflection from the modeling was found to be 20.9  $\mu\text{m}$ . Fig. 3b plots the maximum deflection of the membrane under different flow rates as determined by the modeling as well as a linear regression ( $R^2 = 0.993$ ). For flow rates less than  $\sim 500$   $\mu\text{L/s}$ , the deflection was calculated to be less than a 5  $\mu\text{m}$ , thus explaining why no deflection of the membrane was observed when liquid was pumped into the device at high flow rates using a syringe pump (flow rates  $< 333$   $\mu\text{L/s}$ ).

Fig. 3c shows a visualization of the calculated von Mises stress on the Si membrane under a 2000  $\mu\text{L/s}$  flow rate. This image is characteristic of the stress on the membrane for all flow rates, only the scale changes. The maximum stress was concentrated along the spaces between the pores closest to the edges of the membrane. The maximum von Mises stress for the various flow rates was plotted in Fig. 3d with a linear regression line ( $R^2 = 0.993$ ). At the largest flow rate modeled, the maximum von Mises stress was found to be 680 MPa. The yield strength of Si is 7 GPa and the Young's modulus is 190 GPa, so at 680 MPa the Si will not fail and the deformation will be purely elastic (strain = 0.0039). This was congruent with our observations while manually pipetting 1 mL in the SiMIPA device.

COMSOL was also used to model the 3 x 3 x 0.01 mm<sup>3</sup> PDMS MIPA membrane that was previously used (see supplemental information).<sup>9,11</sup> The simulation data supports previous observations of the poor mechanical stability of the PDMS membrane and emphasizes the need for more the more robust SiMIPA membrane which did not fail at flow rates of  $\sim 2000$   $\mu\text{L/s}$  in the simulations or experimentally.

### ***Isolation of Specific Immune Cell Subpopulations Using SiMIPA***

To verify the specificity in isolation of target immune cell subpopulation using the SiMIPA device, we prepared a heterogeneous mixture of target (Jurkat) and background (THP-1) cells. Here, our test selectively isolated Jurkat cells by adding anti-CD3 PS beads to a 1:1 mixture of Jurkat and THP-1 cells. The anti-CD3 PS beads bound only to the CD3 surface marker expressed by the Jurkat cells (Fig. S3), not by THP-1 cells. The average Jurkat cell-bead conjugation rate was  $2.31 \pm 1.43$  cells/bead (Fig. S3), and this value was used to approximate the number of cells isolated in the device in the typical experiment. When injected via micropipette into the SiMIPA device, the anti-CD3 PS beads became mechanically fixed onto the membrane along with the Jurkat cells bound to them. A representative, composite fluorescent image of the device after washing is seen in Fig. 4. The remaining cells not attached to the beads were free to pass through the membrane. Flushing the device with additional cell culture medium washed away excess unbound cells from the membrane and out through the device outlet. Thus, only the CD3+ Jurkat cells bound to anti-CD3 PS beads were left in the device (Fig. 4d). Trace amounts THP-1 cells remained in the device after washing, as can be seen in Fig. 4d, and we noted that these leftover cells were often found in areas of the device expected to have low flow rates, such as in corners and edges of the chambers. Nonetheless, we found >99% of the cells in the device after washing were the target Jurkat cells, evaluated by fluorescence microscopy and image analysis in ImageJ. Therefore, the SiMIPA was capable of cell subtype isolation from a heterogeneous mixture, discriminating through surface markers expressed by the cells.

### ***In-Device Incubation, Stimulation, and Quantification of T Cell-Secreted Cytokines***

We demonstrated the utility of the SiMIPA device to perform functional immunophenotyping of T-cells by capturing Jurkat cells in the SiMIPA device with CD3-PS

beads, stimulating them with a mixture of PMA and Ionomycin, and quantifying the resulting IL-2 secretion using a no-wash sandwich immunoassay, AlphaLISA. The primary objective of this study is to verify the functionality of the SiMIPA. To this end, we used purified Jurkat cell lines as models of T cells throughout our functional immunophenotyping experiments in lieu of primary or donor-derived PBMC. Avoiding the use of whole blood enables control experiments with the cell culture protocol greatly simplified and reduces sample variation that could occur between donor blood draws. The experimental workflow of the SiMIPA functional immunophenotyping technique is shown in Fig. 5. The protocol of the commercially available AlphaLISA kit, designed for use in a fluorescence microplate reader, was modified for use in the SiMIPA device and custom optical setup (Fig. S2). The total volume and concentration of the reagents were adjusted so that minimum limit of detection (LoD) of the IL-2 assay could be achieved. The standard curve for the modified assay shown in Fig. 6a was obtained by measuring the AlphaLISA signal from SiMIPA devices containing cell culture medium with a known concentration of IL-2. The LoD of the assay was 75.4 pg/mL.

The SiMIPA technique could detect cell-secreted IL-2 from Jurkat cells stimulated with PMA/Ionomycin for 8 hours when as few as 750 CD3-PS beads were captured in the device (Fig. 6b), corresponding to approximately 1800 Jurkat cells. The amount of Jurkat cells isolated in the SiMIPA device was controlled by adjusting the number of beads injected into the device. The average number of Jurkat cells bound to a single CD3-PS bead was 2.41 cells per bead, standard deviation 1.43 (Fig. S3). The measured IL-2 concentration in the SiMIPA device increased as the number of beads injected into the device was increased due to more cells being present to produce IL-2. The maximum number of CD3-PS beads evaluated in this study was 6000 (approx. 14,460 Jurkat cells), at which we estimate half of the membrane holes were plugged by a single bead. If

too many of the pores are blocked by beads, flow through the membrane becomes restricted and could result in insufficient washing. Additionally, a zero-bead condition was examined and showed no IL-2 signal. Therefore, the measured IL-2 in the SiMIPA devices was confirmed to be produced by the T-cells and not as a result of background signal from the reagents or instrumentation.

We further determined that the cell-secreted IL-2 signal could be improved by increasing the amount time the T-cells isolated in the SiMIPA device were allowed to incubate in the PMA/Io stimulant (Fig. 6c). Under normal cell culture conditions (i.e. in culture dish or flask) it is commonly reported in the literature that T-cells will produce IL-2 when incubated with PMA/Io between 4-24 hours. The amount of IL-2 secreted from CD3<sup>+</sup> Jurkat cells captured in the device (6000 beads) increased after the incubation of 4, 6, and 8 hours (Fig. 6c). At each time point, a group of devices containing CD3<sup>+</sup> Jurkat cells but no PMA/Ionomycin was examined. For these devices without PMA/Io, no IL-2 was detected by our assay after the simulation of 4 and 6 hours, however there was a weak signal at 8 hours. T-cells can become activated when they are bound by the CD3 receptor to beads like those used in this study<sup>23</sup>, which would account for the IL-2 measured at this condition. However, we infer that this effect is comparatively much weaker than the PMA/Io in activating the cells, given that the IL-2 signal for the devices containing no PMA/Io can only be measured after 8 hours. The IL-2 concentration measured in the SiMIPA devices was therefore primarily attributed to the PMA/Io stimulant activating the cells to produce IL-2, and the IL-2 signal could be improved by increasing the incubation time.

Using the simulation conditions, we determined to be optimal (6000 beads, 8-hour incubation time), statistically significant ( $P < 0.05$ ) suppression of IL-2 production was observed when the cells were incubated with 1 or 10 ng/mL tacrolimus. At 0.1 and 0.5 ng/mL, the signal

was not statistically different than the 0 ng/mL tacrolimus. Therefore, using SiMIPA we determined that the threshold dose (the lowest concentration at which effects can be seen) of tacrolimus for these cells is 1 ng/mL, indicating that SiMIPA could be used for patients more sensitive to tacrolimus and may only require a low dose. Although 5 repeated measurements were used for each condition in order to minimize noise factors, the standard deviation of each sample was large. The variability of the number of cells captured in the SiMIPA device is likely a contributing factor. Not only is there inherent variability in the number of beads loaded, (estimated based on bead concentration and volume loaded in to the device), there is also variability in the number of cells bound to each bead ( $2.31 \pm 1.43$  cells/bead). Nonetheless, we observed IL-2 production was drastically suppressed at 10 ng/mL compared to 1 ng/mL, indicating that the drug would be most effective in this range. Tacrolimus trough levels are typically prescribed between 5-10 ng/mL depending on patient height, weight, age, kidney function, risk of rejection, and etc., so our observation that the cells used in this study are most suppressed at 10 ng/mL tacrolimus are in line with what is observed in the clinic.<sup>24</sup>

To further validate our results, we incubated Jurkat cells in separate culture flasks with PMA/Io and tacrolimus, and used ELISA to quantify the IL-2 produced after 4-8 hours (Fig. S5). It is worth mentioning that this gold-standard did not integrate any cell sorting functionality and had a total measurement turnaround time of three days: samples were collected on the first day and the ELISA kit protocol required two days. Using SiMIPA, all data down in Fig. 6d was collected in a single day with integrated cell sorting and much less sample used. The ELISA showed similar trends in IL-2 secretion as in SiMIPA: IL-2 production increased with stimulation time and IL-2 production was drastically suppressed at 10 ng/mL tacrolimus. Therefore, we have

validated SiMIPA as an effective platform to assess the secretomic effect of tacrolimus on T-cells separated from a bulk mixture.

While we could see the suppressive effects on T-cell cytokine production at the tacrolimus concentrations we examined, the resolution of SiMIPA should be improved in order to implement the technique in the clinic. Patient outcomes have been improved by maintaining the tacrolimus trough level  $\pm$  1 ng/mL of the physician-prescribed target concentration during inpatient post-transplant care<sup>25</sup>. Therefore, SiMIPA should have at least this resolution in the 1-10 ng/mL range to make clinically useful predictions of optimal dose. Resolution could most readily be improved by improving the LoD of the IL-2 assay used in SiMIPA. While the assay used in this study was optimized for minimum LoD on-chip, the performance was comparatively worse than the rated LoD of the kit if used in a plate reader ( $\sim$ 2 ng/mL). With improved sensitivity SiMIPA would be able to discern between smaller tacrolimus concentration intervals, and the assay time and number of cells needed would likely be reduced, also further improving experimental throughput.

To improve our future SiMIPA assay, we consider several strategies; First, the device chamber volume can be reduced so that the new design allows the secreted cytokines to be more spatially confined and enhances the local chemiluminescence to improve measurement sensitivity. Second, the AlphaLISA assay conditions may be optimized by increasing the assay incubation time, adjusting the detection antibody concentrations, and implementing a 2 or 3-step assay protocol suggested by the manufacturer (PerkinElmer Inc, Waltham, MA). Third, the PMT could be replaced with a single photon counter to improve the signal-to-noise ratio in detecting photoemission by optically excited AlphaLISA reagents. Finally, the measurement throughput could be achieved by adopting the recent 4-plex no-wash AlphaLISA assay that enables users to

simultaneously monitor the secretion of INF- $\gamma$  and IL-17 in addition to IL-2. These additional cytokines are also of interest for predicting allograft rejection<sup>4,5</sup>.

Although our current study did not involve whole blood sample, our group's prior work<sup>26</sup> successfully demonstrated the direct isolation, enrichment, enumeration, and immunophenotyping of CD14<sup>+</sup> monocytes from whole blood using a PDMS version of the MIPA device using a similar protocol to the one used here. The previous work achieved ~98% purity for monocytes isolated from whole blood. Our future clinical study will apply the SiMIPA technology for monitoring the immunophenotypes of CD3<sup>+</sup> T-cells in patients' blood samples. Sharing a common membrane design with the previous PDMS MIPA devices, the Si devices developed in this study are anticipated to yield satisfactory performance in T-cell isolation from whole blood. Once the platform is capable of more precisely assessing T-cell IL-2 production in the 1-10 ng/mL range and simultaneously assessing the secretion of multiple cytokines, clinical study using patient-derived samples is possible in order to correlate SiMIPA predictions of tacrolimus efficacy to patient outcomes.

## **CONCLUSION**

In this study, a microfluidic device was developed that could perform sorting, incubation, and cell-secreted cytokine quantification of target cells from a heterogeneous mixture. The microfluidic device was fabricated using a combination of silicon micromachining and soft lithography processes such that production of the device was highly scalable. Using a single 100 mm wafer, 172 devices could be fabricated with >99% yield. The device was able to sort target cells from a background population with excellent purity (>98%) and culture the cells for at least 8 hours. The

device was compatible with a commercially available no-wash immunoassay so that functional immunophenotyping could be performed on-chip. When isolated in the device, cells were confirmed to be producing IL-2 as measured by the assay in response to chemical stimuli. The IL-2 concentration signal could be improved by increasing the number of cells isolated in the device and the total time the cells were incubated with the chemical stimulant. The scalable manufacturing techniques used to produce the device allowed for sufficiently large experimental throughput to perform immunomodulatory drug screening on isolated immune cell subsets at multiple drug concentration conditions. Suppressed IL-2 production was observed at 1 and 10 ng/mL concentrations of tacrolimus in the cell culture environment on-chip within clinically relevant trough concentration ranges. By circumventing laborious cell separation by flow cytometry and slow measurement turnaround time of current gold-standard assays, we demonstrated that the device enables a rapid, *in vitro* approach to personalized immunosuppressive drug therapy.

### **Author's contributions**

RN developed and fabricated the SiMIPA technology, conducted the multiphysics modeling, planned the experiments, and supervised the experimental work. AS developed SiMIPA protocols and planned and carried out the experiments. RN and AS wrote and revised the manuscript. NM carried out cell-purity experiments and revised the manuscript. MTC developed the optical setup, assisted in the multiphysics modeling, and provided general support. YS provided support with cell cultures and revised the manuscript. JF and KK supervised the research and revised the manuscript.

## Acknowledgements

The authors would like to thank Walker McHugh, Kelli McDonough, Skyler Reitberg, and Dr. Timothy Cornell of the Cornell Group (University of Michigan) for their assistance with cell culturing and for use of their laboratory space and to thank Dr. Mengxi Wu for taking the SEM image of their device. This study was supported by the National Institutes of Health (Grant No. R01 HL119542-01A1). R. N. thanks the Michigan Institute for Clinical & Health Research for support under the Postdoctoral Translational Scholars Program by Grant Number 2UL1TR000433 from the National Center for Advancing Translational Sciences. This material is based upon work supported by the National Science Foundation Graduate Research Fellowship under Grant No. 1256260. Any opinion, findings, and conclusions or recommendations expressed in this material are those of the authors(s) and do not necessarily reflect the views of the National Science Foundation. The content is solely the responsibility of the authors and does not necessarily represent the official views of NCATS or the National Institutes of Health. Portions of this work were performed at the Lurie Nanofabrication Facility at the University of Michigan.

## REFERENCES

- 1 C. E. Staatz and S. E. Tett, *Clin. Pharmacokinet.*, 2015, **54**, 993–1025.
- 2 W. J. Jusko, W. Piekoszewski, G. B. Klintmalm, M. S. Shaefer, M. F. Hebert, A. A. Piergies, C. C. Lee, P. Schechter and Q. A. Mekki, *Clin. Pharmacol. Ther.*, 1995, **57**, 281–290.
- 3 J. J. Jia, B. Y. Lin, J. J. He, L. Geng, D. Kadel, L. Wang, D. D. Yu, T. Shen, Z. Yang, Y. F. Ye, L. Zhou and S. Sen Zheng, *World J. Gastroenterol.*, 2014, **20**, 11363–11369.
- 4 O. Millán, L. Rafael-Valdivia, E. Torrademé, A. López, V. Fortuna, S. Sánchez-Cabus, Y. López-Púa, A. Rimola and M. Brunet, *Cytokine*, 2013, **61**, 556–64.

- 5 O. Millán and M. Brunet, *Clin. Biochem.*, 2016, **49**, 338–346.
- 6 H. T. Maecker, J. P. McCoy and R. Nussenblatt, *Nat. Rev. Immunol.*, 2012, **12**, 191–200.
- 7 W. Chen, N.-T. Huang, X. Li, Z. T. F. Yu, K. Kurabayashi and J. Fu, *Front. Oncol.*, 2013, **3**, 98.
- 8 H. T. Maecker, J. P. McCoy and R. Nussenblatt, *Nat. Rev. Immunol.*, 2012, **12**, 471–471.
- 9 W. Chen, N. T. Huang, B. Oh, R. H. W. Lam, R. Fan, T. T. Cornell, T. P. Shanley, K. Kurabayashi and J. Fu, *Adv. Healthc. Mater.*, 2013, **2**, 965–975.
- 10 M. Brunet, O. Millán López and M. López-Hoyos, *Ther. Drug Monit.*, 2016, **38**, S21–S28.
- 11 N.-T. Huang, W. Chen, B.-R. Oh, T. T. Cornell, T. P. Shanley, J. Fu and K. Kurabayashi, *Lab Chip*, 2012, **12**, 4093.
- 12 C. Wyatt Shields IV, C. D. Reyes and G. P. López, *Lab Chip*, 2015, **15**, 1230–1249.
- 13 W. Al-Faqheri, T. H. G. Thio, M. A. Qasaimeh, A. Dietzel, M. Madou and A. Al-Halhouli, *Microfluid. Nanofluidics*, 2017, **21**, 102.
- 14 L. R. Volpatti and A. K. Yetisen, *Trends Biotechnol.*, 2014, **32**, 347–350.
- 15 C. W. Shields, K. A. Ohiri, L. M. Szott and G. P. López, *Cytom. Part B - Clin. Cytom.*, 2017, **92**, 115–125.
- 16 E. K. Sackmann, A. L. Fulton and D. J. Beebe, *Nature*, 2014, **507**, 181–189.
- 17 K. E. Petersen, *Proc. IEEE*, 1982, **70**, 420–457.
- 18 R. Holdich, S. Kosvintsev, I. Cumming and S. Zhdanov, *Philos. Trans. R. Soc. A Math. Phys. Eng. Sci.*, 2006, **364**, 161–174.
- 19 W. Chen, R. H. W. Lam and J. Fu, *Lab Chip*, 2012, **12**, 391–5.
- 20 Y. Jiang, Z. Yu, X. Huang, R. Chen, W. Chen, Y. Zeng, C. Xu, H. Min, N. Zheng and X. Cheng, *Microfluid. Nanofluidics*, 2018, **22**, 40.
- 21 S. W. Lee and S. S. Lee, *Microsyst. Technol.*, 2008, **14**, 205–208.
- 22 E. Berthier, E. W. K. Young and D. Beebe, *Lab Chip*, 2012, **12**, 1224–37.
- 23 J. A. Ledbetter, L. E. Gentry, C. H. June, P. S. Rabinovitch and A. F. Purchio, *Mol. Cell. Biol.*, 1987, **7**, 650–6.
- 24 TACROLIMUS (FK506) LEVEL (FOR TRANSPLANT PATIENTS), [https://www.childrensmn.org/references/lab/chemistry/tacrolimus-level-\(for-transplant-patients-only\).pdf](https://www.childrensmn.org/references/lab/chemistry/tacrolimus-level-(for-transplant-patients-only).pdf), (accessed 18 July 2017).
- 25 A. Zarrinpar, D. K. Lee, A. Silva, N. Datta, T. Kee, C. Eriksen, K. Weigle, V. Agopian, F. Kaldas, D. Farmer, S. E. Wang, R. Busuttil, C. M. Ho and D. Ho, *Sci. Transl. Med.*, 2016, **8**, 333ra49.

26. W. Chen, N.T. Huang, B.R. Oh, R.H.W. Lam, R. Fan, T.T. Cornell, T.P. Shanley, K. Kurabayashi, and J. Fu, *Adv. Health. Mat.*, 2013, **2**, 965-975.

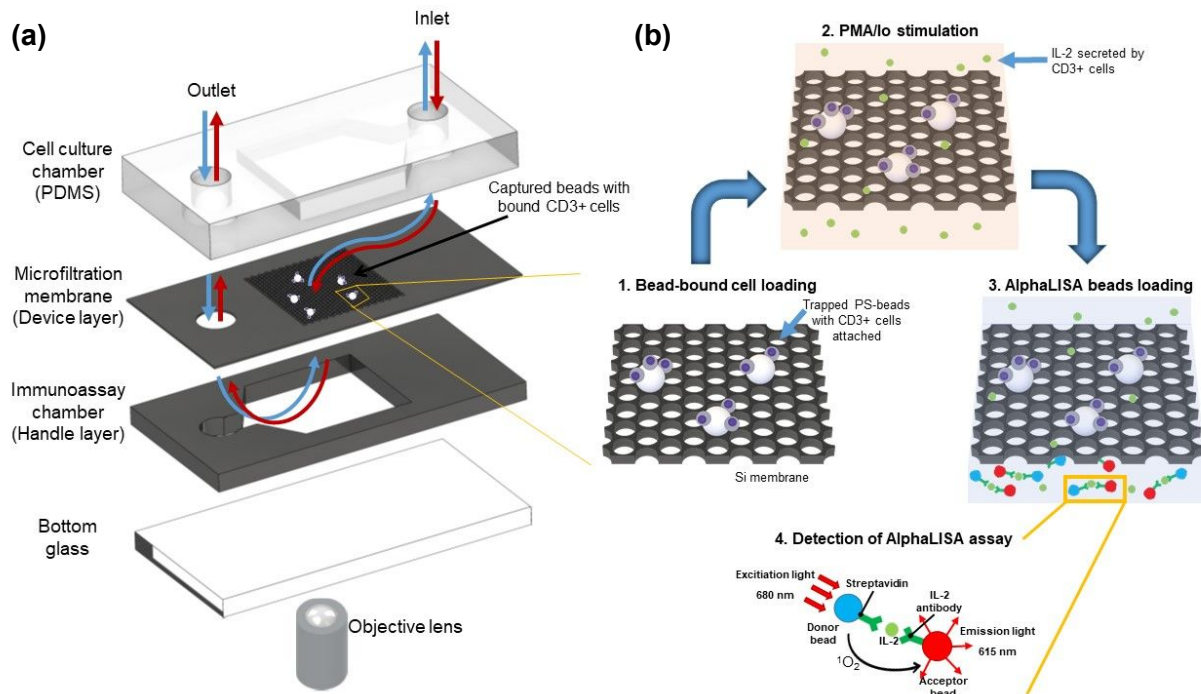


**Fig. 1.** T-cell isolation and functional immunophenotyping using the SiMIPA device. (a) Schematic of the micro-fabricated device showing bottom glass layer (borofloat glass wafer), immunoassay chamber (handle layer of SOI wafer), microfiltration membrane layer (device layer of SOI wafer) and cell culture chamber fabricated using PDMS soft lithography. The size of the cell culture chamber was 3 mm (L:length) x 3 mm (W:width) x 100  $\mu\text{m}$  (H:height), the size of the immunoassay chamber was 3 mm x 3 mm x 525  $\mu\text{m}$ , and the size of the of the PDMS cell culture chamber was 3 mm x 3mm x 100  $\mu\text{m}$ . The SiMIPA device was positioned over an objective lens that both focused 680 nm laser light through the bottom glass and into the immunoassay chamber, and to collect the chemiluminescent light that was subsequently emitted by the AlphaLISA assay. (b) Schematic showing the on-chip immunophenotyping assay used throughout this study: (1) Beads with bound T-cells are filtered from the sample loaded into the device and mechanically fixed on the microfiltration membrane. (2) PMA/Io stimulation of cells (3) Loading of AlphaLISA reagents into the device and incubation. (4) Detection of cell-secreted IL-2 by excitation of AlphaLISA assay.

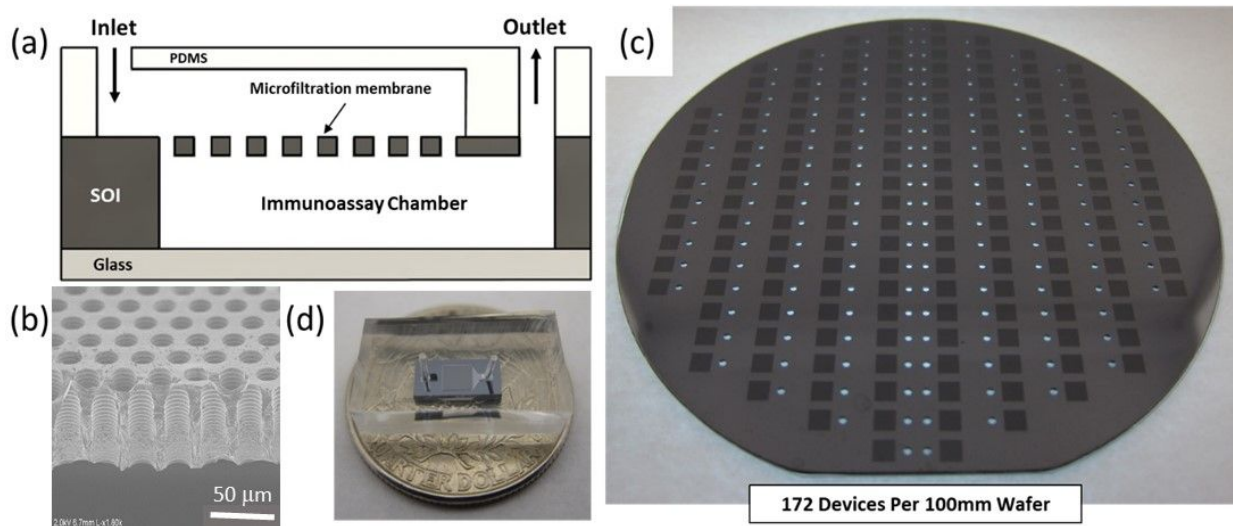


**Fig. 2.** SiMIPA device microfabrication and features. (a) Cross-section illustration of the SiMIPA device. The top PDMS defines the top chamber and the inlet and out. The SOI wafer makes up the microfiltration membrane (device layer) and the immunoassay chamber (handle layer). The glass wafer provides a window for visualizing the immunoassay chamber and quantifying secreted cytokines using AlphaLISA. Illustration is not drawn to scale. (b) Scanning electron microscope (SEM) image of the microfiltration membrane which consists of 11,443 holes (20  $\mu\text{m}$  diameter) in a hexagonal lattice with a center-to-center spacing of 30  $\mu\text{m}$ , which yields a 40% porosity in the device layer. (c) Individual SiMIPA device shown with a U.S. quarter for reference. (d) Full wafer after finished microfabrication and anodic bonding showing 172 devices on the 100 mm SOI wafer.

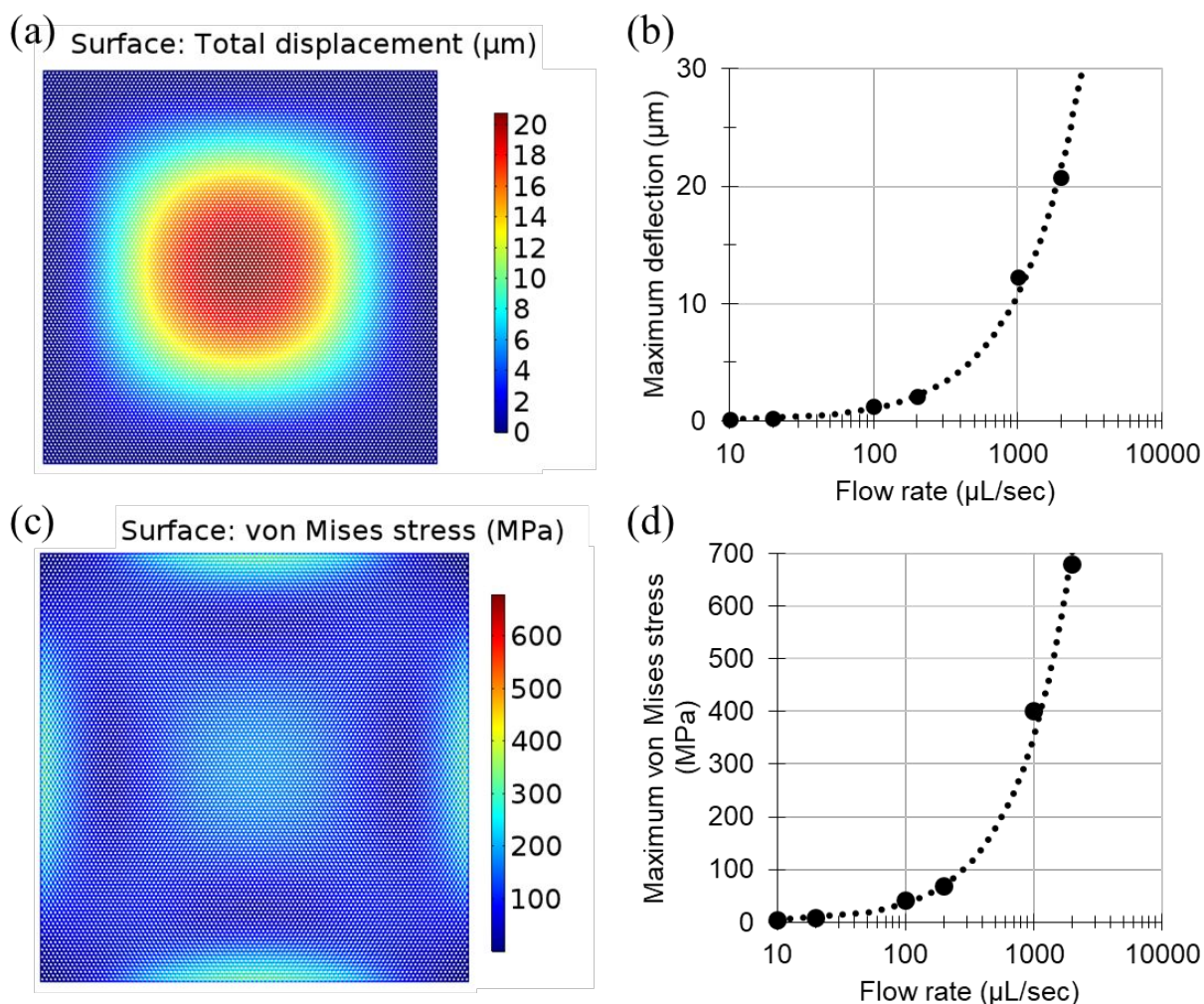


**Fig. 3.** Finite element modeling of the deflection of the SiMIPA microporous membrane under fluid flow. (a) Rendering from COMSOL showing the deflection of a membrane with 20  $\mu\text{m}$  holes under a 2000  $\mu\text{L}/\text{sec}$  flow rate. (b) A plot of the simulated deflection of a  $3 \times 3 \times 0.05 \text{ mm}^3$  Si membrane under different flow rates while the  $3 \times 0.05 \text{ mm}^2$  faces are fixed. The membrane has a hexagonal lattice of pores through the 0.05 mm thick membrane where the center-to-center spacing is equal 30  $\mu\text{m}$ . The linear regression line intercepts at  $y = 0$  and has  $R^2 = 0.9925$ . (c) Rendering from COMSOL showing the von Mises stress on a membrane with 20  $\mu\text{m}$  holes under a 2000  $\mu\text{L}/\text{sec}$  flow rate. (d) A plot of the simulated maximum von Mises stress observed on a  $3 \times 3 \times 0.05 \text{ mm}^3$  membrane under different flow rates while the  $3 \times 0.05 \text{ mm}^2$  faces are fixed. The membrane has a hexagonal lattice of pores through the 0.05 mm thick membrane where the center-to-center spacing is 30  $\mu\text{m}$ . The linear regression line intercepts at  $y = 0$  and has  $R^2 = 0.9925$ .

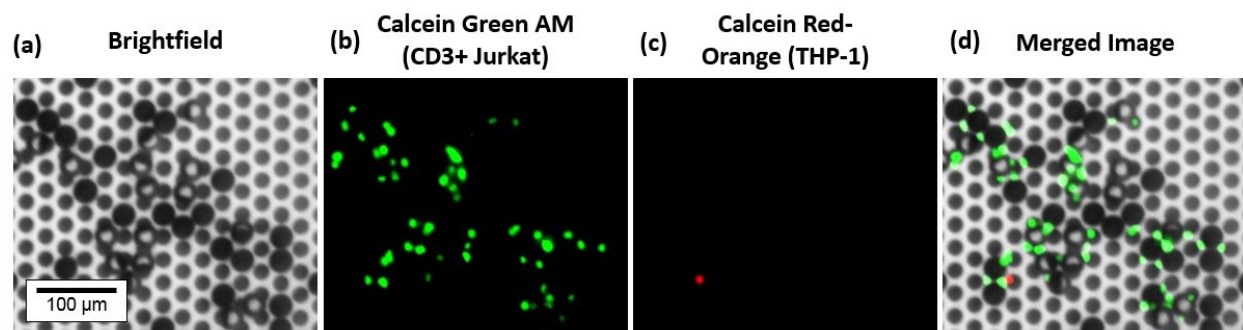


**Fig. 4.** Brightfield, fluorescence, and merged brightfield and fluorescence images of CD3-PS beads, Jurkat cells (green) and trace THP-1 cells (red) isolated on the microporous membrane of the SiMIPA device. CD-PS beads were transparent and appear as gray or black spheres. Jurkat cells were stained with Calcein AM Green, THP-1 cells were stained with Calcein AM Red-Orange.

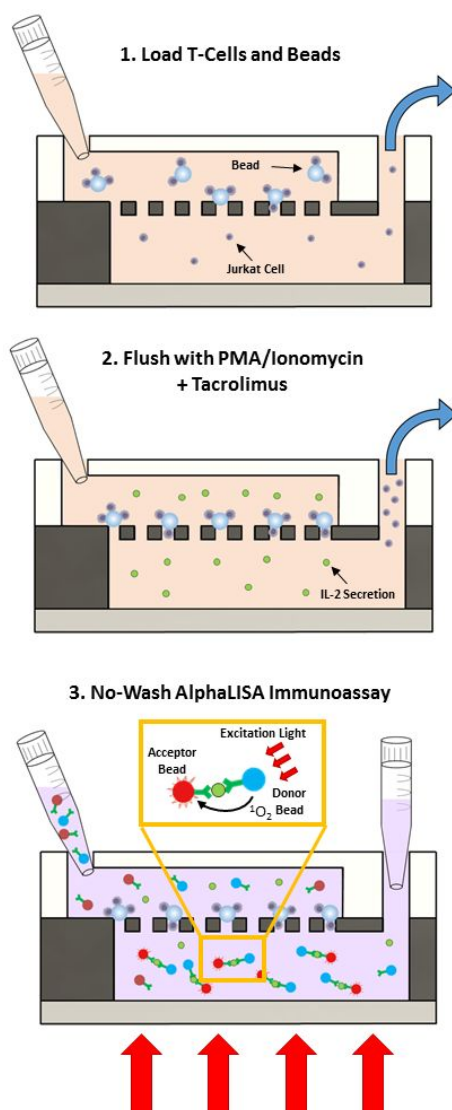


**Fig. 5.** Experimental workflow of SiMIPA platform. (1) Conjugated cells and beads are pipetted into the device inlet using a standard micropipette. (2) Device is flushed with cell culture medium containing a cocktail of PMA/Ionomycin and Tacrolimus. Cells not bound to beads are washed away while cells bound to beads are mechanically isolated on the microporous silicon membrane. (3) After incubation, no-wash AlphaLISA reagents are loaded into the device. A pipette tip placed in the outlet acts as a reservoir to prevent any sample or reagents from escaping. The concentration of IL-2 in the device is determined by measuring the intensity of the chemiluminescent light emitted from the device at 615 nm following excitation by 680 nm laser light. The insert shows the excitation light (red arrows) interacting with the donor beads (blue circles), which releases  $O_2$  in order to generate emission from the acceptor beads (red circles). Both the donor beads and acceptor beads are bound to the target, IL-2. All illustrations are not to scale.

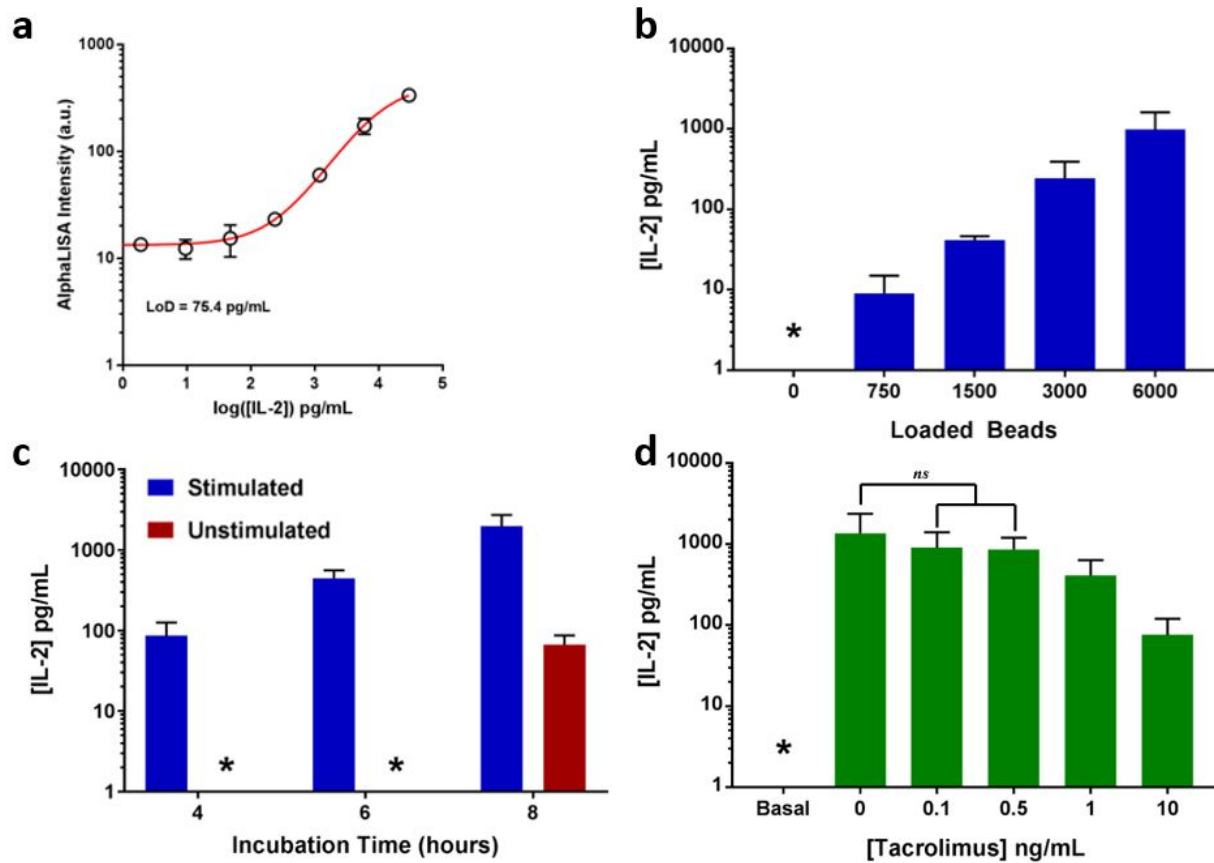


**Fig. 6.** Quantification of cell secreted cytokines in SiMIPA device using homogeneous chemiluminescence-based assay. For all data, (\*) indicates a signal too low to be quantified. One-tailed heteroscedastic t-test was used to compare all data sets and, unless specified as *ns* ( $P > 0.05$ ), all combinations had a  $p < 0.05$  a) Standard curve for human IL-2. b) Measured IL-2 concentration in the device for increasing number of beads loaded into the device. c) Measured IL-2 concentration in the device after loading 6000 beads and incubating for a certain time. d) Measured IL-2 concentration in the device for devices loaded with 6000 beads and incubated in a cocktail of PMA/Ionomycin and a given concentration of tacrolimus.